HHS Public Access

Author manuscript

Nat Chem. Author manuscript; available in PMC 2011 May 01.

Published in final edited form as:

Nat Chem. 2010 November ; 2(11): 962–966. doi:10.1038/nchem.858.

Recognition-Mediated Activation of Therapeutic Gold Nanoparticles Inside Living Cells

CHAEKYU KIM[1,†], **SARIT S. AGASTI**[1,†], **ZHENGJIANG ZHU**[1], **LYLE ISAACS**[2], and **VINCENT M. ROTELLO**[1,*]

[1]Department of Chemistry, University of Massachusetts, 710 North Pleasant Street, Amherst, MA 01003, USA

[2]Department of Chemistry and Biochemistry, University of Maryland, College Park, Maryland 20742, USA

Abstract

Supramolecular chemistry provides a versatile tool for the organization of molecular systems into functional structures and the actuation of these assemblies for applications through the reversible association between complementary components. Application of this methodology in living systems represents a significant challenge due to the chemical complexity of cellular environments and lack of selectivity of conventional supramolecular interactions. Herein, we present a host-guest system featuring diaminohexane-terminated gold nanoparticles (AuNP-NH_2) and complementary cucurbit[7]uril (CB[7]). In this system, threading of CB[7] on the particle surface reduces the cytotoxicity of AuNP-NH_2 through sequestration of the particle in endosomes. Intracellular triggering of the therapeutic effect of AuNP-NH_2 was then achieved via the administration of 1-adamantylamine (ADA), removing CB[7] from the nanoparticle surface and triggering the endosomal release and concomitant *in situ* cytotoxicity of AuNP-NH_2. This supramolecular strategy for intracellular activation provides a new tool for potential therapeutic applications.

Supramolecular chemistry uses non-covalent interactions to provide controlled assembly of molecular building blocks. 1, 2, 3, 4, 5, 6 By virtue of reversible noncovalent interactions (e.g. hydrogen bonding, ion-ion, pi-pi stacking and van der Waals interactions), supramolecular complexes are inherently dynamic in nature and highly selective toward other complementary guest molecules through these various weak and reversible

---

*rotello@chem.umass.edu.

†These authors contributed equally to this work

Author contributions

C.K., S.S.A. and V.M.R. conceived and designed the experiments. C.K., S.S.A. and Z.Z performed the experiments. C.K., S.S.A., Z.Z., L.I. and V.M.R. analyzed the data. C.K., S.S.A., Z.Z., and V.M.R. wrote the paper.

Supplementary Information

Synthesis of diaminohexane-terminated thiol ligand, construction of AuNP-NH_2, MALDI-MS characterization, ICP-MS sample preparation and other characterization methods.

Competing financial interests

None

interactions.7 As a result of the modularity and the reversibility, supramolecular systems can be engineered to assemble and disassemble spontaneously in response to a range of triggers. 2, 1, 8

The versatility of supramolecular chemistry makes this strategy a promising tool for biomedical science. A number of host-guest supramolecular systems (e.g. nanovalves and artificial molecular machines) have been reported for the delivery of drugs and other therapeutic materials. 9, 10, 11 The engineering of such systems has been achieved principally through the design of molecular recognition partners, thereby fine tuning the molecular recognition event to meet the demands of specific applications. A number of synthetic receptors including cucurbit[n]uril (CB[n]),9, 12 cyclodextrins,13, 14 cyclophanes, 15 calixarenes,16 and crown ethers17,18 have been used for this purpose. Of these host systems, the cucurbit[n]uril (CB[n]) family of macrocyclic receptors is particularly useful due to their well defined structure and recognition properties coupled with their ability to form stable host-guest inclusion complexes with a wide variety of guest molecules in aqueous media.19, 20, 21 This capability has been exploited for the creation of delivery vectors, including the encapsulation of platinum drugs inside the cavity of CB[7] to increase the stability of the drugs in biological environments.22, 23, 24,25 In another example, the strong affinity of spermine towards CB has been utilized to tailor a DNA delivery vector for enhanced transfection efficiency and target specificity.26, 27 In these systems, the properties of the guest molecule have been modified as a result of the supramolecular complexation with the host molecules, enhancing delivery properties.

In addition to modification of molecular properties, supramolecular chemistry provides the capability of actuation.9, 11, 28, 29 Engineering of host-guest systems to function inside the cell provides a potentially powerful strategy for the regulation of therapeutics. We present here a supramolecular system featuring complementary diaminohexane-terminated gold nanoparticles (AuNP-NH_2) and cucurbit[7]uril (CB[7]) that form a non-toxic assembly that is readily taken up by the cells (Fig. 1). This host-guest complex can be disassembled intracellularly by the orthogonal guest molecule 1-adamantylamine (ADA) that features a very high affinity to CB[7]. Intracellular removal of CB[7] from the nanoparticle surface results in a endosomal escape by the AuNP-NH_2, thereby activating the cytotoxicity of AuNP-NH_2 and hence inducing cell death (Fig. 1). This result presents a new strategy for triggering therapeutic systems through the use of competitive interactions of orthogonally presented guest molecules, with immediate advantages in dosage control and potential utility for dual-targeting therapies.

Results and discussion

The therapeutic component of the system is provided by AuNP-NH_2 (2.5 ± 0.4 nm core size) featuring a self-assembled monolayer of diaminohexane terminated thiol ligands (Fig. 1a).30 The terminal diaminohexane moiety both renders the particle cytotoxic (vide infra) and serves as a recognition unit for the formation of host-guest inclusion complex with CB[7]. The association constant of this diamine-CB[7] complexation process is ~ 10^8 M^{-1} and the complex has been shown to be stable under biological conditions.24, 31, The complexation between AuNP-NH_2 and CB[7] was investigated using NMR titration

experiments as shown in Fig. 2. As the ratio of CB[7]/ AuNP-NH_2 increases, the peaks for the methylene groups of AuNP-NH_2-CB[7] are shifted upfield relative to those of AuNP-NH_2. This behavior indicates that terminal diaminohexane units were encapsulated inside the shielding zone of CB[7] cavity as AuNP-NH_2-CB[7] complex forms. 32 At the ratio of 1:40 (AuNP-NH_2:CB[7]), the signal shift of the methylene groups was completely saturated, revealing the number of CB[7] around a single nanoparticle is ~40. According to the thermogravimetric analysis (TGA), the number of diaminohexane-terminated ligands on a single nanoparticle estimated is ~43 (Supplementary Information Fig. S7), indicating almost complete encapsulation of diaminohexane units by CB[7].

The AuNP-NH_2-CB[7] complex was further characterized through transmission electron microscopy (TEM) as shown in Fig. 2b. TEM images taken after uranyl acetate staining showed that each gold nanoparticle was encapsulated by CB[7]. The average overall diameter of the nanoparticles calculated from the TEM image of AuNP-NH_2-CB[7] is 11.4 ± 0.8 nm, which is in good agreement with the hydrodynamic diameter observed by DLS experiment (12.1 ± 0.8 nm). In addition, no size change or aggregation of nanoparticles was observed from UV-Vis spectra of the nanoparticles, indicating no morphological change after complexation (see Supplementary Information Fig. S4).

The competitive unsheathing of the AuNP-NH_2-CB[7] complex by ADA (commonly used as an antiviral or anti-Parkinsonian drug 33, 34, 35) was confirmed using NMR and matrix-assisted laser desorption/ionization mass spectroscopy (MALDI-MS). Addition of ADA triggered the release of CB[7] from nanoparticles through creation of the more favorable 1:1 ADA-CB[7] complexes ($K_a = 1.7 \times 10^{12}$).31 As expected, the shifted resonance signals of the methylene groups of the ligands induced by complexation with CB[7] were fully recovered as soon as ADA was added (see Supplementary Information Fig. S2). In MALDI-MS, the AuNP-NH_2 and AuNP-NH_2-CB[7] exhibit characteristic ion peaks at m/z 479.44 and 1641.8 respectively, corresponding to the molecular ion (M^+) of [HS-NH_2] and [HS-NH_2-CB[7]]. After addition of ADA, the ion peak of [HS-NH_2-CB[7]] disappeared and a new peak of [ADA-CB[7]] appeared, indicating efficient complexation/decomplxation process (see Supplementary Information Fig. S3).

The cellular uptake of the nanoparticles was quantified using inductively coupled plasma mass spectrometry (ICP-MS). ICP-MS analysis revealed that the total amount of the nanoparticles taken up by the cells was nearly identical for AuNP-NH_2 and AuNP-NH_2-CB[7] (Fig. 3). TEM analysis of the cells was employed to evaluate the impact of CB[7] complexation on the intracellular fate/localization of the nanoparticles. As shown in Supplementary Information Fig. S5a and S5b, after 3 h incubation, both AuNP-NH_2 and AuNP-NH_2-CB[7] are trapped within vesicular structures morphologically consistent with endosomes. This observation is consistent with the behavior observed with other cationic nanoparticles, as reported in our previous work.36, 37 After 24 h of incubation, however, AuNP-NH_2 particles had escaped from the endosome and were dispersed in the cytosol (Fig. 4a). In contrast, AuNP-NH_2-CB[7] particles remained sequestered in the endosome with no free particles observed in the cytosol. (Fig. 4b and Supplementary Information Fig. S6) after the same period. Significantly, incubation of AuNP-NH_2-CB[7]-treated cells with ADA for 24 h resulted in the escape of a substantial number of particles into the cytosol (Fig. 4c),

consistent with intracellular transformation of AuNP-NH_2-CB[7] to AuNP-NH_2 via dethreading.

Polyamine functionalized macromolecules 38, 39, 40 and nanoparticles 41, 42, 43, 44 interact strongly with cell membranes and subcellular compartments, resulting in membrane disruption and cytotoxicity. Complexation of AuNP-NH_2 with CB[7] should attenuate the positive charge of the particle surfaces, reducing the ability of the particles to disrupt membranes (including the endosomal) and hence lower toxicity. The cytotoxicity of AuNP-NH_2 and AuNP-NH_2-CB[7] was investigated in the human breast cancer MCF-7 cell line using an Alamar blue assay. The AuNP-NH_2-CB[7] complex was substantially less toxic as compared to AuNP-NH_2. After 24 h incubation, AuNP-NH_2 exhibited cytotoxicity with 1.3 μM of IC_{50} value (Fig. 5a). On the other hand, AuNP-NH_2-CB[7] complex did not inhibit cell proliferation at concentrations ≤ 50 μM under the same experimental conditions, presumably arising from sequestration of the particle in the endosome. Significantly, when the free thiol ligand was added to the cells at concentrations consistent with those used in the study (80 μM, corresponding to the same per-ligand concentration as 2 μM nanoparticle) toxicity was observed with both threaded and unthreaded ligand, demonstrating the modulation of ligand toxicity on the particle.

Given the observed intracellular dethreading of AuNP-NH_2-CB[7] with ADA and concomitant release from the endosome, the endosomal escape of the nanoparticles after ADA treatment raises the possibility that toxicity of the AuNP-NH_2-CB[7] complex can be triggered by ADA. To test this hypothesis MCF-7 cells were incubated with 2 μM of AuNP-NH_2-CB[7] in culture medium for 3h, to allow endocytosis of nanoparticles.45 Cells were then washed three times with PBS buffer, and then ADA was added to the culture medium. Cells were then incubated for an additional 24 h. Cells treated with AuNP-NH_2 and AuNP-NH_2-CB[7] alone exhibited 34 % and 100 % cell viability after 24 h incubation, respectively (Fig. 5b). Treatment with 0.4 mM ADA led to 40 % cell viability, approaching the level of lethality observed for the AuNP-NH_2 control (Fig. 5b). The result indicates that ADA acts as an effective trigger for the competitive release of CB[7] from particles within the cell, with attendant activation of cytotoxicity.

In summary, we have demonstrated the use of synthetic host-guest chemistry to provide triggered activation of a therapeutic system via competitive complexation. This approach provides a potential strategy for the construction of synthetic host-guest supramolecular systems capable of complex and sophisticated behavior within living cells. Triggering therapeutic systems through the use of competitive interactions of orthogonally presented guest molecules can be potentially useful for dual-targeting therapies, i.e. targeting of both host and guest component. This provides the potential for orthogonal (“effector/trigger”) drug delivery and therapeutic activation46, 47 that would be capable of achieving higher levels of site specific activity, and reduced amounts of collateral damage. Currently, we are exploring this strategy *in vivo* and thoroughly considering issues (e.g. the practical use of ADA) related to the real-world application of this system.

METHODS

Synthesis of AuNP-NH_2 and ICP-MS sample preparation are described in supplementary information. ^{1}H NMR spectra of the nanoparticles and the complexes were recorded on a Bruker AVANCE 400 at 400 MHz. MALDI-MS analyses were performed using a Bruker Omniflex time-of-flight mass spectrometer. UV-Vis spectra were recorded on Hewlett-Packard 8452A spectrophotometer. Dynamic light scattering (DLS) was measured by Zetasizer Nano ZS.

MCF-7 cells were grown in a cell culture flask using low glucose Dulbecco's Modified Eagle Medium supplemented with 10% fetal bovine serum (FBS) at 37°C in a humidified atmosphere of 5% CO_2. For cytotoxicity tests involving AuNP-NH_2 and AuNP-NH_2-CB[7], MCF-7 cells were seeded at 20,000 cells in 0.2 ml per well in 96-well plates 24 h prior to the experiment. During experiment old media was replaced by different concentrations of AuNP-NH_2 and AuNP-NH_2-CB[7] in serum containing media and the cells were incubated for 24 h at 37°C in a humidified atmosphere of 5 % CO_2. The cells were then completely washed with PBS buffer for three times and 10% Alarmar blue in serum containing media was added to each well and further incubated at 37 °C for 4 h. The cell viability was then determined by measuring the fluorescence intensity at 570 nm using a SpectraMax M5 microplate spectrophotometer. Curves were fitted by DoseRep function in Origin 8. For measuring cytotoxicity of AuNP-NH_2-CB[7] upon adding ADA, MCF-7 cells were seeded at 20,000 cells per well in 96-well plate 24 h prior to the experiment. The old medium was replaced by 2 μM of AuNP-NH_2-CB[7] in medium containing serum and incubated for 3h. The cells were then completely washed with PBS buffer for three times and different concentration (0, 0.2 and 0.4 mM) of ADA in serum containing media was added to the cells and further incubated at 37 °C for 24 h. The cell viability was then determined by using Alamar blue assay.

TEM samples of nanoparticles were prepared by placing one drop of the desired nanoparticles solution (1~3 μM) on to a 300-mesh Cu grid coated with carbon film, followed by 2 % of uranyl acetate staining for 15 min. These samples were analyzed and photographed using JEOL 100S electron microscopy. For a preparation of cellular TEM samples, MCF-7 cells were seeded and incubated on 15 mm diameter Theramanox® coverslips (Nalge Nunc International, NY) placed in 24 well plates at amount of 100,000 cells in 1 ml of serum containing media for 24 h prior to the experiment. The media was replaced by 0.5 ml of 2 μM AuNP-NH_2 or AuNP-NH_2-CB[7] in serum containing media and incubated for 24 h. The medium containing the gold nanoparticles was then discarded and the cells were completely washed with PBS buffer for three times. The cells were then fixed in 2 % glutaraldehyde with 3.75 % sucrose in 0.1 M sodium phosphate buffer (pH 7.0) for 30 min and then washed with 0.1 M PBS containing 3.75% sucrose three times over 30 min. They were postfixed in 1 % osmium tetroxide with 5 % sucrose in 0.05 M sodium phosphate buffer solution (pH 7.0) for 1 hr and the rinsed with distilled water three times. They were dehydrated in a graded series of acetone (10 % step), and embedded in epoxy resin. The resin was polymerized at 70 °C for 12 h. Ultrathin sections (50 nm) obtained with a Reichert Ultracut E Ultramicrotome and imaged under a JEOL 100S electron microscopy. For the preparation of TEM samples for the cells treated with AuNP-NH_2-CB[7] and

subsequent incubation with ADA, pre-seeded MCF-7 cells on 15 mm diameter Theramanox® coverslips were treated by AuNP-NH_2-CB[7] (2 μM) for 3h. After washing three times with PBS buffer, the cells were further incubated with ADA (0.4 mM) in serum containing media for 24 h.

Supplementary Material

Refer to Web version on PubMed Central for supplementary material.

Acknowledgements

We thank David Solfiell for his assistance in preparing this manuscript. SSA acknowledges a graduate school fellowship. This work was supported by the NIH (GM077173, VR), and L.I. thanks the National Science Foundation (CHE-0615049 and CHE-0914745) for financial support.

References

1. Lehn JM. Toward self-organization and complex matter. Science. 2002; 295:2400–2403. [PubMed: 11923524]
2. Lehn JM. From supramolecular chemistry towards constitutional dynamic chemistry and adaptive chemistry. Chem. Soc. Rev. 2007; 36:151–160. [PubMed: 17264919]
3. Reinhoudt DN, Crego-Calama M. Synthesis beyond the molecule. Science. 2002; 295:2403–2407. [PubMed: 11923525]
4. Yaghi OM, et al. Reticular synthesis and the design of new materials. Nature. 2003; 423:705–714. [PubMed: 12802325]
5. Lehn, JM. Supramolecular Chemistry: Concepts and Perspectives. VCH; New York: 1995.
6. Dankers PYW, Harmsen MC, Brouwer LA, Van Luyn MJA, Meijer EW. A modular and supramolecular approach to bioactive scaffolds for tissue engineering. Nature Mater. 2005; 4:568–574. [PubMed: 15965478]
7. Hennig A, Bakirci H, Nau WM. Label-free continuous enzyme assays with macrocycle fluorescent dye complexes. Nat. Methods. 2007; 4:629–632. [PubMed: 17603491]
8. Klajn R, et al. Dynamic hook-and-eye nanoparticle sponges. Nature Chem. 2009; 1:733–738. [PubMed: 21124361]
9. Angelos S, Yang Y-W, Patel K, Stoddart JF, Zink JI. pH-responsive supramolecular nanovalves based on cucurbit[6]uril pseudorotaxanes. Angew. Chem. Int. Edit. 2008; 47:2222–2226.
10. Angelos S, et al. pH Clock-Operated Mechanized Nanoparticles. J. Am. Chem. Soc. 2009; 131:12912–12914. [PubMed: 19705840]
11. Coti KK, et al. Mechanised nanoparticles for drug delivery. Nanoscale. 2009; 1:16–39. [PubMed: 20644858]
12. Lee HK, et al. Vesicle formed by amphiphilc cucurbit[6]uril: Versatile, noncovalent modification of the vesicle surface, and multivalent binding of sugar-decorated vesicles to lectin. J. Am. Chem. Soc. 2005; 127:5006–5007. [PubMed: 15810820]
13. Park C, Oh K, Lee SC, Kim C. Controlled release of guest molecules from mesoporous silica particles based on a pH-responsive polypseudorotaxane motif. Angew. Chem. Int. Edit. 2007; 46:1455–1457.
14. Du L, Liao S, Khatib HA, Stoddart JF, Zink JI. Controlled-Access Hollow Mechanized Silica Nanocontainers. J. Am. Chem. Soc. 2009; 131:15136–15142. [PubMed: 19799420]
15. Hayashida O, Uchiyama M. Multivalent macrocyclic hosts: Histone surface recognition, guest binding, and delivery by cyclophane-based resorcinarene oligomers. J. Org. Chem. 2007; 72:610–616. [PubMed: 17221981]
16. Sansone F, et al. DNA condensation and cell transfection properties of guanidinium calixarenes: Dependence on macrocycle lipophilicity, size, and conformation. J. Am. Chem. Soc. 2006; 128:14528–14536. [PubMed: 17090036]

17. Weimann DP, Winkler HDF, Falenski JA, Koksch B, Schalley CA. Highly dynamic motion of crown ethers along oligolysine peptide chains. Nature Chem. 2009; 1:573–577. [PubMed: 21378938]
18. Darwish IA, Uchegbu IF. The evaluation of crown ether based niosomes as cation containing and cation sensitive drug delivery systems. Int. J. Pharm. 1997; 159:207–213.
19. Lee JW, Samal S, Selvapalam N, Kim H-J, Kim K. Cucurbituril homologues and derivatives: New opportunities in supramolecular chemistry. Acc. Chem. Res. 2003; 36:621–630. [PubMed: 12924959]
20. Kim K, et al. Functionalized cucurbiturils and their applications. Chem. Soc. Rev. 2007; 36:267–279. [PubMed: 17264929]
21. Lagona J, Mukhopadhyay P, Chakrabarti S, Isaacs L. The cucurbit[n]uril family. Angew. Chem. Int. Edit. 2005; 44:4844–4870.
22. Wheate NJ, et al. Multi-nuclear platinum complexes encapsulated in cucurbit[n]uril as an approach to reduce toxicity in cancer treatment. Chem. Commun. 2004:1424–1425.
23. Jeon YJ, et al. Novel molecular drug carrier: encapsulation of oxaliplatin in cucurbit[7]uril and its effects on stability and reactivity of the drug. Org. Biomol. Chem. 2005; 3:2122–2125. [PubMed: 15917899]
24. Wheate NJ. Improving platinum(II)-based anticancer drug delivery using cucurbit[n]urils. J. Inorg. Biochem. 2008; 102:2060–2066. [PubMed: 18653238]
25. Wheate NJ, Buck DP, Day AI, Collins JG. Cucurbit[n]uril binding of platinum anticancer complexes. Dalton Trans. 2006:451–458. [PubMed: 16395444]
26. Lim YB, et al. Self-assembled ternary complex of cationic dendrimer, cucurbituril, and DNA: Noncovalent strategy in developing a gene delivery carrier. Bioconjugate Chem. 2002; 13:1181–1185.
27. Kim SK, et al. Galactosylated cucurbituril-inclusion polyplex for hepatocyte-targeted gene delivery. Chem. Commun. 2010; 46:692–694.
28. Angelos S, Yang YW, Khashab NM, Stoddart JF, Zink JI. Dual-Controlled Nanoparticles Exhibiting AND Logic. J. Am. Chem. Soc. 2009; 131:11344–11346. [PubMed: 19624127]
29. Ghosh S, Isaacs L. Biological Catalysis Regulated by Cucurbit[7]uril Molecular Containers. J. Am. Chem. Soc. 2010; 132:4445–4454. [PubMed: 20210325]
30. Templeton AC, Wuelfing MP, Murray RW. Monolayer protected cluster molecules. Acc. Chem. Res. 2000; 33:27–36. [PubMed: 10639073]
31. Liu SM, et al. The cucurbit[n]uril family: Prime components for self-sorting systems. J. Am. Chem. Soc. 2005; 127:15959–15967. [PubMed: 16277540]
32. Lee JW, Ko YH, Park SH, Yamaguchi K, Kim K. Novel pseudorotaxane-terminated dendrimers: Supramolecular modification of dendrimer periphery. Angew. Chem. Int. Edit. 2001; 40:746–749.
33. Davies WL, et al. Antiviral Activity of 1-Adamantanamine (Amantadine). Science. 1964; 144:862–863. [PubMed: 14151624]
34. Maassab HF, Cochran KW. Rubella Virus - Inhibition in Vitro by Amantadine Hydrochloride. Science. 1964; 145:1443–1444. [PubMed: 14172640]
35. Hagan JJ, Middlemiss DN, Sharpe PC, Poste GH. Parkinson's disease: Prospects for improved drug therapy. Trends Pharmacol. Sci. 1997; 18:156–163. [PubMed: 9184476]
36. Zhu ZJ, Ghosh PS, Miranda OR, Vachet RW, Rotello VM. Multiplexed Screening of Cellular Uptake of Gold Nanoparticles Using Laser Desorption/Ionization Mass Spectrometry. J. Am. Chem. Soc. 2008; 130:14139–14143. [PubMed: 18826222]
37. Kim CK, et al. Entrapment of Hydrophobic Drugs in Nanoparticle Monolayers with Efficient Release into Cancer Cells. J. Am. Chem. Soc. 2009; 131:1360–1361. [PubMed: 19133720]
38. Godbey WT, Wu KK, Mikos AG. Poly(ethylenimine) and its role in gene delivery. J. Controlled Release. 1999; 60:149–160.
39. Leroueil PR, et al. Wide varieties of cationic nanoparticles induce defects in supported lipid bilayers. Nano Lett. 2008; 8:420–424. [PubMed: 18217783]

40. Fischer D, Bieber T, Li YX, Elsasser HP, Kissel T. A novel non-viral vector for DNA delivery based on low molecular weight, branched polyethylenimine: Effect of molecular weight on transfection efficiency and cytotoxicity. Pharm. Res. 1999; 16:1273–1279. [PubMed: 10468031]
41. Ghosh PS, Kim CK, Han G, Forbes NS, Rotello VM. Efficient Gene Delivery Vectors by Tuning the Surface Charge Density of Amino Acid-Functionalized Gold Nanoparticles. ACS Nano. 2008; 2:2213–2218. [PubMed: 19206385]
42. Lovric J, et al. Differences in subcellular distribution and toxicity of green and red emitting CdTe quantum dots. J. Mol. Med-Jmm. 2005; 83:377–385.
43. Goodman CM, McCusker CD, Yilmaz T, Rotello VM. Toxicity of gold nanoparticles functionalized with cationic and anionic side chains. Bioconjugate Chem. 2004; 15:897–900.
44. Fuller JE, et al. Intracellular delivery of core-shell fluorescent silica nanoparticles. Biomaterials. 2008; 29:1526–1532. [PubMed: 18096220]
45. Verma A, et al. Surface-structure-regulated cell-membrane penetration by monolayer-protected nanoparticles. Nature Mater. 2008; 7:588–595. [PubMed: 18500347]
46. Taylor SK, et al. Triggered Release of an Active Peptide Conjugate from a DNA Device by an Orally Administrable Small Molecule. Angew. Chem. Int. Edit. 2009; 48:4394–4397.
47. Sarkar D, et al. Dual cancer-specific targeting strategy cures primary and distant breast carcinomas in nude mice. Proc. Natl. Acad. Sci. U.S.A. 2005; 102:14034–14039. [PubMed: 16172403]

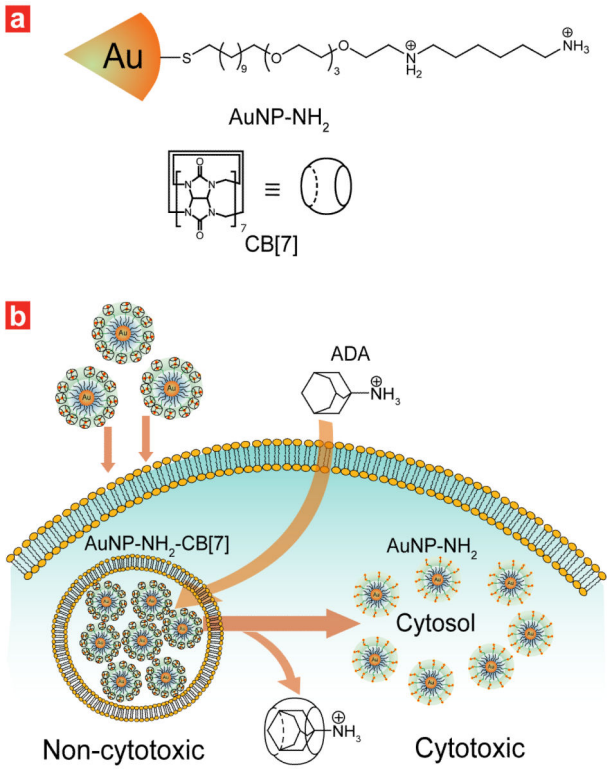

Figure 1. Structure of gold nanoparticle and use of intracellular host-guest complexation to trigger nanoparticle cytotoxicity

(a) Structure of diaminohexane-terminated gold nanoparticle (AuNP-NH_2) and cucurbit[7]uril (CB[7]). (b) Activation of AuNP-NH_2-CB[7] cytotoxicity by dethreading of CB[7] from the nanoparticle surface by ADA.

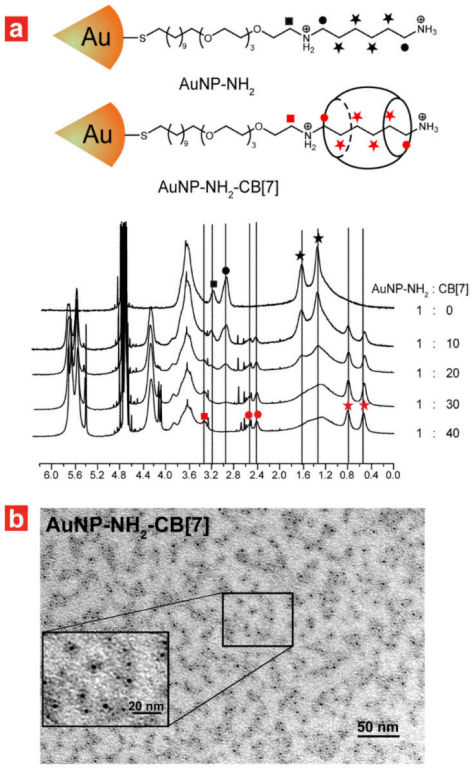

Figure 2. NMR titration and TEM of AuNP-NH_2-CB[7] complex

(a) The resonance signals for the methylene groups (• and ★) of AuNP-NH_2-CB[7] were shifted upfield, relatively to those in AuNP-NH_2. (b) TEM image of AuNP-NH_2-CB[7] complex. TEM sample was prepared by placing the desired AuNP-NH_2-CB[7] solution (3 μM) on to a Cu grid coated with carbon film, followed by 2 % of uranyl acetate staining for 15 min. Increase of electron density of organic layer on nanoparticle after binding with CB[7] afford the organic shell of AuNP-NH_2-CB[7] enough to be visualized in the TEM image. Organic shell on AuNP-NH_2 was not observed in the same TEM sample preparation.

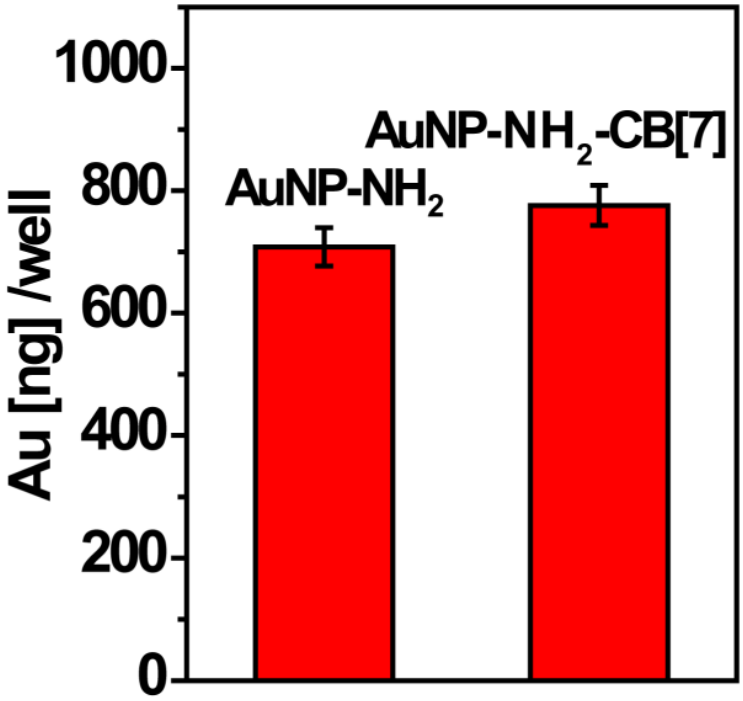

Figure 3. Cellular uptake of the gold nanoparticles

Quantification of the amount of gold present in cells. Samples were analyzed by ICP-MS to determine the amount of gold in MCF-7 cell after 3 h incubation with 0.5 μM of AuNP-NH_2 and AuNP-NH_2-CB[7]. Both particles showed almost same cellular uptake. Cellular uptake experiments with each gold nanoparticle were repeated 3 times, and each replicate was measured 5 times by ICP-MS. Error bars represent the standard deviations of these measurements.

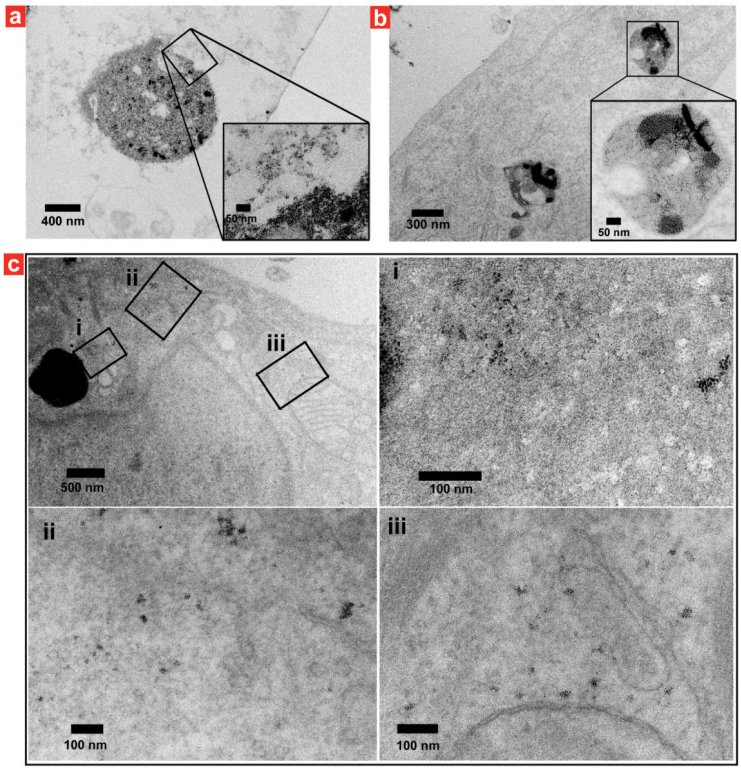

Figure 4. Intracellular localization of the gold nanoparticles

TEM images of cross sectional MCF-7 cells incubated for 24 h with 2 μM (a) AuNP-NH_2 and (b) AuNP-NH_2-CB[7]. Significant amount of AuNP-NH_2 is present in the cytosol, however most of the AuNP-NH_2-CB[7] seems to be trapped in organelles such as endosome. (c) TEM images of cross sectional MCF-7 cells incubated for 3 h with 2 μM of AuNP-NH_2-CB[7] and then further incubation with ADA for 24 h. In the intracellular environment ADA transforms AuNP-NH_2-CB[7] to AuNP-NH_2, which then escaped from the endosome and observed to be dispersed in the cytosol. i, ii and iii are the magnified sections from the first panel of part (c).

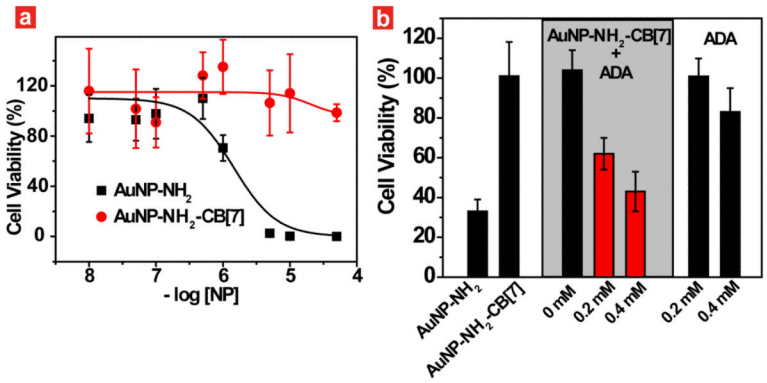

Figure 5. Cytotoxicity of AuNP-NH_2 and AuNP-NH_2-CB[7] and modulating cytotoxicity of the gold nanoparticles

(a) Cytotoxicity of AuNP-NH_2 and AuNP-NH_2-CB[7] measured by Alamar blue assay after 24 h incubation in MCF-7. IC_{50} of AuNP-NH_2 was 1.3 μM and no cytotoxicity of AuNP-NH_2-CB[7] was observed up to 50 μM. (b) Triggering cytotoxicity using ADA. After 3h incubation of AuNP-NH_2-CB[7] (2 μM) in MCF-7 cell, different concentrations (0, 0.2 and 0.4 mM) of ADA in medium added and further incubated at 37 °C for 24 h. The cell viability was then determined by using an Alamar blue assay. As controls, cell viability of AuNP-NH_2 and AuNP-NH_2-CB[7] was measured after 24 h incubation (34 % and 100%, respectively). Cell viability experiments were performed as triplicate and the error bars represent the standard deviations of these measurements.